ELSEVIER

Materials Chemistry and Physics 62 (2000) 153–157

MATERIALS CHEMISTRY AND PHYSICS

www.elsevier.com/locate/matchemphys

The effects of microcrystalline silicon film structure on low-high-low band-gap thin film transistor

Chun-Yen Chang*, Yeong-Shyang Lee, Tiao-Yuan Huang, Po-Sheng Shih, Chiung-Wei Lin

Department of Electronics Engineering & Institute of Electronics, National Chiao Tung University, Hsinchu 300, Taiwan

Received 14 April 1999; received in revised form 2 July 1999; accepted 2 July 1999

Abstract

The effects of hydrogenated microcrystalline silicon (μc-Si:H) film with various crystalline factors on thin-film transistors (TFTs) with low-high-low band gap structure are studied. Compared to hydrogenated amorphous silicon (a-Si:H) TFT with conventional inverted-stagger structure, the device with μc-Si:H film of high crystalline factor in the active channel depicts improved interfacial active layer near the gate insulator interface as well as the later-grown bulk active layer, resulting in improved device parameters including field effect mobility, threshold voltage, subthreshold swing and ON-current. While a-Si:H film of low crystalline factor and high-band-gap is proposed for the source and drain offset regions in the new device to prevent the band-to-band tunneling, thus alleviates the high OFF-current inherent in conventional μc-Si:H thin-film transistors, resulting in an improved ON/OFF current ratio.

Keywords: Thin-film transistor (TFT); Microcrystalline; Amorphous; Crystalline factor

1. Introduction

Hydrogenated amorphous silicon thin-film transistors (a-Si:H TFT's) are widely used as the pixel switching elements in active-matrix liquid-crystal displays (AMLCDs) [1]. However, a-Si:H TFT's suffer from a low field-effect carrier mobility and high instability associated with the a-Si:H channel, which lead to low current drivability and severe device degradation during device operation. Many methods have thus been proposed for improving the turn-on characteristics of TFT's, including the use of double gate structure [2], short channel device [3], and vertical structure [4]. However, these methods normally require complicated processing and are difficult to implement. On the other hand, polycrystalline silicon (poly-Si) TFT's are known to depict better current drivability while suffering a large OFF-state leakage current. To alleviate the high OFF-state current in poly-Si TFTs, devices with a horizontal offset structure have been proposed [5]. The conventional horizontal offset structure suppresses the OFF-state carrier conduction effectively by reducing the drain electric field near the gate edge. However, it requires a large device area to incorporate the offset region. In addition, complicated processing such as light-dose ion implantation and the accompanying high annealing temperature, may be required in horizontal offset structure, except for the structure which employs field plate. Recently, new crystalline material with higher band mobility than that of a-Si:H, namely, microcrystalline silicon (μc-Si:H), has been proposed to achieve superior current drivability. However, the OFF-state current remains high, resulting in a marginal ON/OFF current ratio of only five orders of magnitude or less [6–9].

More recently, we have proposed a high-performance TFT with a novel vertical offset structure, whose channel region and offset region are composed of μc-Si:H and a-Si:H films, respectively [10–12]. Compared to the conventional inverted-stagger a-Si:H TFT with a single high-band-gap a-Si:H layer, the proposed TFT features the insertion of a thin low-band-gap μc-Si:H layer at the semiconductor/insulator (i.e., high-band-gap a-Si:H/SiN_x) interface. The high quality, low-band-gap μc-Si:H film is used to enhance the current drivability of this novel device. While the high-band-gap a-Si:H layer is retained to suppress the OFF-state leakage current to a level comparable to that of conventional a-Si:H TFT's. In addition, this novel device employs a heavily doped low-band-gap n^+ a-Si:H layer as its source/drain ohmic contacts to ensure a good ohmic contact between semiconductor and metal.

*Corresponding author.

0254-0584/00/$ – see front matter
PII: S0254-0584(99)00174-1

In this paper, we focus on the effects of μc-Si:H channel film with different crystalline factors (CF) on device performance. Because the fabrication process of the proposed TFTs is similar to that of the conventional inverted-stagger a-Si:H TFTs with the offset region (i.e., high-band-gap undoped a-Si:H) stacks vertically above the channel, the area of our new device with low-high-low band gap structure is smaller than that of a conventional horizontal offset device. This will increase the pixel density of TFTs array, making it attractive for future high-definition-television system (HDTV) applications. Finally, it should be noted that all the films employed in our devices are deposited under low temperature ($\leq$300°C), and the fabrication process is simple and inexpensive with the potential of high reliability.

2. Experimental

The device structure of low-high-low band-gap TFT is shown schematically in Fig. 1. The fabrication process is similar to that of a conventional inverted-stagger a-Si:H TFT's except for the insertion of a low-band-gap μc-Si:H film between the gate insulator and the undoped a-Si:H film. Briefly, a 250 nm-thick aluminum film was deposited by evaporation on silicon wafers that were previously coated with a 500-nm-thick thermal oxide layer. The aluminum film was then patterned to form the gate electrode by photolithography and wet etching. Next, a silicon nitride (SiN_x) gate insulator, a compound channel layer consisting of a low-band-gap μc-Si:H and a high-band-gap undoped a-Si:H, and a low-band-gap n^+ a-Si:H film were deposited consecutively by a plasma-enhanced chemical vapor deposition (PECVD) system without breaking the vacuum. The gas mixtures for SiN_x, undoped a-Si:H and n^+ a-Si:H films were ($SiH_4 + NH_3 + N_2$), ($SiH_4 + H_2$), and ($SiH_4 + PH_3$), respectively. The thickness for SiN_x, undoped a-Si:H, and n^+ a-Si:H films was 300, 140, and 70 nm, respectively. The SiN_x film was deposited under the condition of 300°C, 27.78 mw cm^{-2}, and 1 Torr, while the undoped and n^+ a-Si:H films were deposited at 250°C, 25 mw cm^{-2}, 0.3 Torr. While the thickness of μc-Si:H films was fixed at 25 nm, samples with various $[H_2]/\{[SiH_4] + [H_2]\}$ flow rate ratios were fabricated to study its effects. Specifically, μc-Si:H films were deposited at 250°C, 25 mw cm^{-2} and 0.55 Torr using a $[H_2]/\{[SiH_4] + [H_2]\}$ flow rate ratio of 980 sccm/(23 sccm + 980 sccm) for 97.7%-diluted film and 980 sccm/(9 sccm + 980 sccm) for 99.1%-diluted film, respectively. Finally, a 250 nm-thick aluminum film was again evaporated on the grown films and patterned to form source and drain electrodes. CF_4 plasma etching was then used to define the active device region and to remove the unwanted n^+ a-Si:H layer.

The nominal channel width (W) for the completed devices is 120 mm, while the nominal channel length (L) is 10 mm. All devices were then annealed at 200°C in N_2 ambient for 25 min to form good ohmic contacts. The electrical properties of the completed devices were measured by a HP4145B semiconductor parameter measurement system with a PC. The crystallinity of μc-Si:H and a-Si:H films was analyzed by Raman scattering spectra. Optical bandgap (E_{opt}) was determined from a Tauc plot of the optical absorption coefficient in ~0.4 μm-thick a-Si:H and μc-Si:H films, which were deposited under identical conditions, except for the flow rate of hydrogen and silane gas.

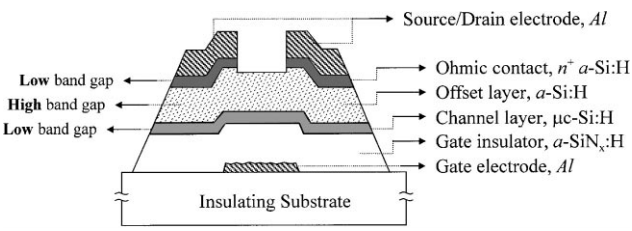

Fig. 1. Schematic diagram of the thin-film transistor with low-high-low band gap structure.

3. Results and discussion

In this paper, we focus on the effects of μc-Si:H channel films with various crystalline factors on the device performance of TFTs with low-high-low band-gap structure. As shown in Table I, the crystalline factor (CF) of a-Si:H/μc-Si:H films prepared with various deposition conditions is different. Fig. 2 shows the Raman spectra, which are very sensitive in revealing film quality, of three films deposited on glass under various gas ratios. The crystallinity of μc-Si:H and a-Si:H films was analyzed by Raman scattering spectra. It was observed that there are two bands around 520 cm^{-1} Raman shift (i.e., crystalline-Si peak) and 480 cm^{-1} Raman shift (i.e., amorphous-Si peak) for the three films. The crystalline factor (CF) was estimated by the

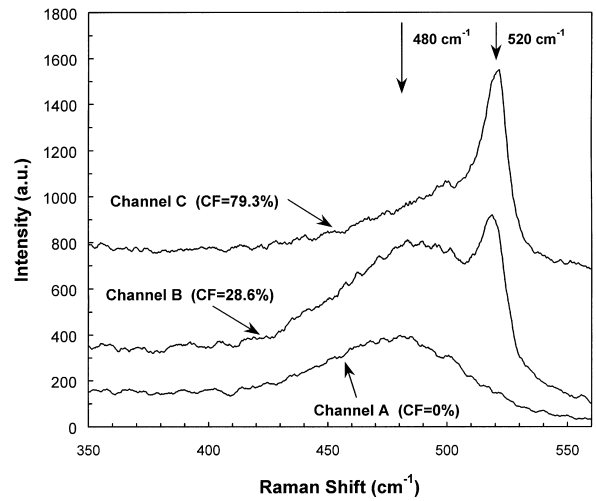

Fig. 2. Raman spectra of hydrogenated amorphous/microcrystalline silicon films with various crystalline factors (CF).

Table 1
Crystalline factor (CF) of channel films prepared by various deposition conditions

Channel films	Gas source (sccm)	H_2 dilution ratio	Optical bandgap E_{opt} (eV)	Crystalline factor CF (%)
A (CF = 0%) (a-Si:H)	SiH_4/H_2 (23/23)	50%	1.71	0%
B (CF = 28.6%) (μc-Si:H)	SiH_4/H_2 (9/980)	99.1%	1.61	28.6%
C (CF = 79.3%) (μc-Si:H)	SiH_4/H_2 (23/980)	97.7%	1.39	79.3%

ratio of the area around 520 cm^{-1} peak to the total area extracted from the Raman spectra. From the Raman spectra shown in Fig. 2, the crystalline factor of undoped a-Si:H film used as the channel film is found to be 0%. While the crystalline factor of 97.7%-diluted μc-Si:H film is 79.3%, which is higher than that of 99.1%-diluted μc-Si:H film (CF ∼ 28.6%). In addition, the optical bandgap (E_{opt}) of these channel films is also shown in Table 1. It is observed that the optical bandgap is lower for films with higher quality, compared to films with lower quality. In other words, films with higher crystalline factor have lower optical bandgap. In addition, E_{opt} of n^+ a-Si:H film used for all devices is ∼1.48 eV. In accordance with the optical bandgap of channel/offset/contact films, the new TFT structure as shown in Fig. 1 is named ''low-high-low band-gap structure''.

Fig. 3 shows the transfer characteristics for devices with a-Si:H/μc-Si:H channel film of various crystalline factors at $V_{ds} = 1$ V. All devices depict good characteristics including small threshold voltage and sharp transition region. As shown in Fig. 3, the presence of μc-Si:H channel film with high crystalline factor (CF) improves the ON-state characteristics, while the presence of a high-band-gap a-Si:H offset film (CF = 0%) suppresses the OFF-state leakage current caused by band-to-band tunneling (BBT). For convenience, we denote the channel films with 50%-diluted ($E_{opt} \sim 1.71$ eV), 99.1%-diluted ($E_{opt} \sim 1.61$ eV) and 97.7%-diluted ($E_{opt} \sim 1.39$ eV) a-Si:H/μc-Si:H films as A (CF = 0%), B (CF = 28.6%) and C (CF =79.3%), respectively. As shown in Fig. 3, device with channel C (CF = 79.3%) depicts improved ON-state and OFF-state currents, compared to device with channel B (CF = 28.6%). We believe the improvement is mainly due to the discontinuity of valence band between low-band-gap channel layer and high-band-gap offset layer. A larger difference in the valence band discontinuity between low-band-gap channel layer and high-band-gap offset layer results in more effective hole confinement, thus suppresses the OFF-state leakage current [13]. The band discontinuities between low-band-gap channel layer (i.e., μc-Si:H) and high-band-gap offset layer (i.e., a-Si:H) for devices with channel C (CF = 79.3%) and B (CF = 28.6%) are ∼0.32 eV and ∼0.10 eV, respectively. Therefore, the effectiveness of suppressing the OFF-state leakage current in device with channel C (CF = 79.3%) is much more effective than that in device with channel B (CF = 28.6%). In general, devices with channel C (CF = 79.3%) and channel B (CF = 28.6%) show higher current driving capabilities than device with channel A (CF = 0%). The improvement in current driving capability is determined by the quality of channel films, i.e., the crystalline factor of channel films.

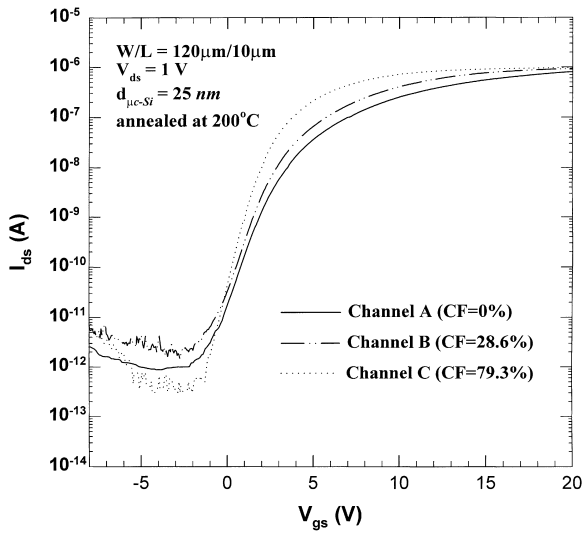

Fig. 3. Transfer characteristics at small V_{ds} (=1 V) for devices with various channel films.

From Fig. 3, the ON-state current increases from 6.55 mA/m for the device with channel A (CF = 0%) to 7.44 mA/m for device with channel B (CF = 28.6%). The increase is even more dramatic for device with channel C (CF = 79.3%) (i.e., to 8.26 mA/m). This confirms that devices with μc-Si:H channel film of high crystalline factor can not only improve the OFF-state characteristics but also improve the driving current. The higher ON-current density is believed to be due to less bulk trap density. To confirm this hypothesis, we have measured and deduced the density of deep gap states (N_{deep}) according to the equation: $N_{deep} = C_{ins}S(qkt)^{-1}$, where S, C_{ins} is the subthreshold swing and gate insulator capacitor respectively. We indeed found that the density of deep gap states (N_{deep}) decreases from 7.34×10^{12} cm^{-2} eV^{-1} for device with channel A (CF = 0%) to 6.28×10^{12} cm^{-2} eV^{-1} for device with channel B (CF = 28.6%), and to 4.79×10^{12} cm^{-2} eV^{-1} for device with channel C (CF = 79.3%). The density of deep gap states (N_{deep}) is dependent on the quality of a-Si:H or μc-Si:H films, and the optical band gap (E_{opt}) is also dependent on the quality of a-Si:H or μc-Si:H films, as shown in Fig. 4 and Table 1 respectively.

Fig. 5 shows the dependence of subthreshold swing (S) on crystalline factor (CF) of channel film. A trend similar to that of the density of deep gap states (N_{deep}) is also observed.

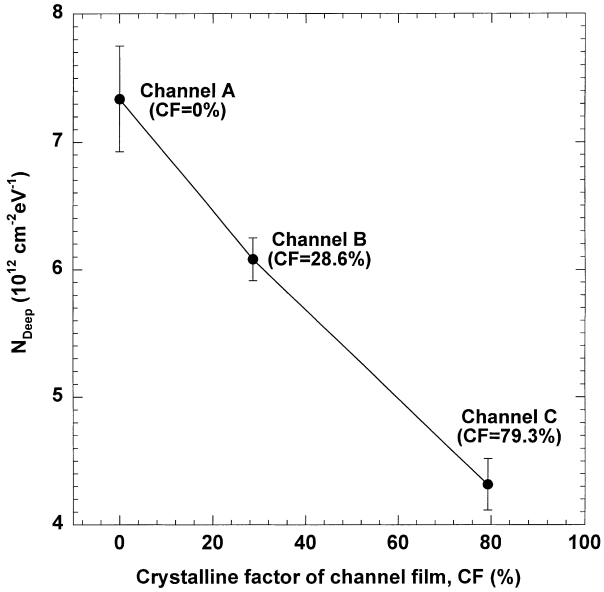

Fig. 4. Densities of deep gap states for devices with channel films having various crystalline factors (CF).

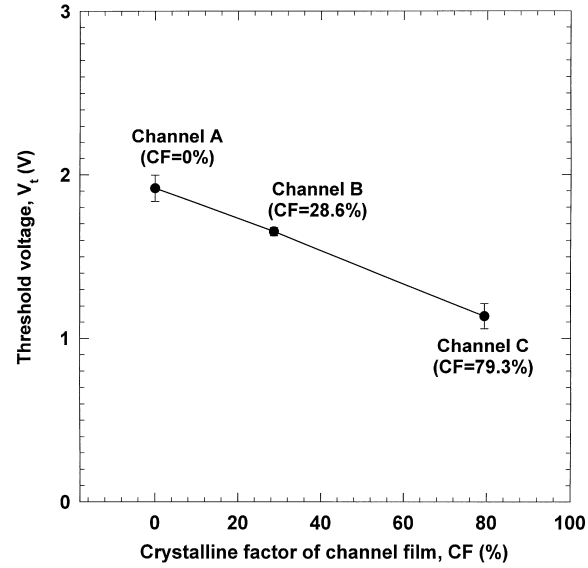

Fig. 6. Threshold voltages for devices with channel films having various crystalline factors (CF).

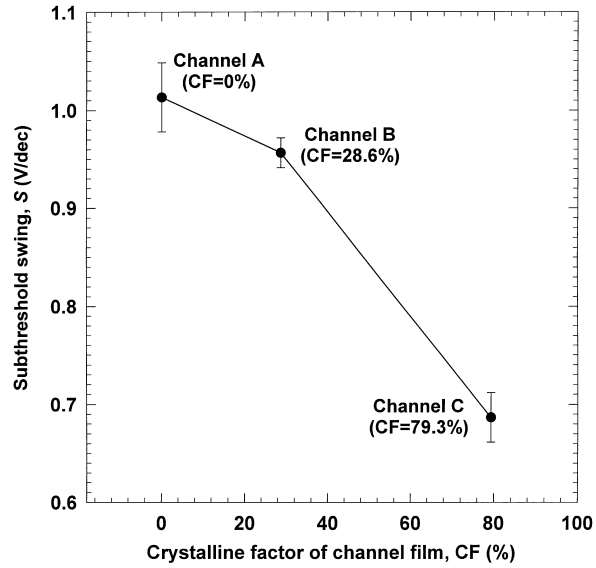

Fig. 5. Subthreshold swings for devices with channel films having various crystalline factors (CF).

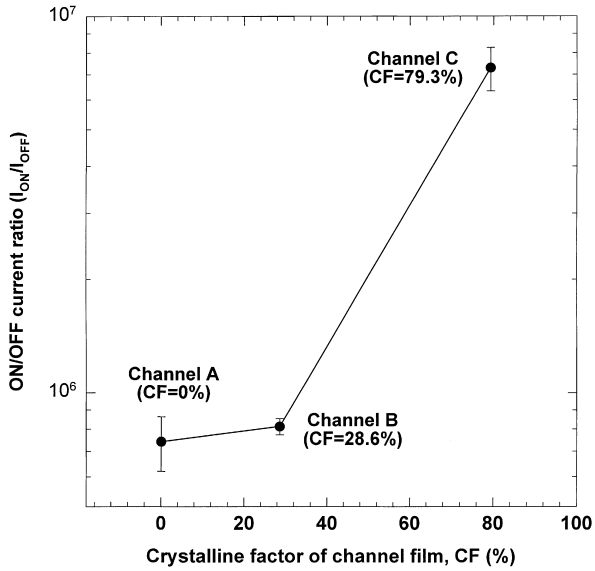

Fig. 7. ON/OFF current ratios for devices with channel films having various crystalline factors (CF).

The subthreshold swing decreases from 1.01 V/dec for device with a-Si:H channel A whose CF = 0% to 0.96 V/dec for device with μc-Si:H channel B whose CF = 28.6%, and to 0.68 V/dec for device with μc-Si:H channel C whose CF = 79.3%. In addition, smaller threshold voltages (V_t) are obtained for our novel devices as shown in Fig. 6, i.e., 1.91, 1.65 and 1.08 V for devices with channel A (CF = 0%), B (CF = 28.6%), and C (CF = 79.3%), respectively.

Fig. 7 shows that the device performance does improve by inserting a high quality (i.e., high crystalline factor), low-band-gap μc-Si:H film for the new devices with low-high-low band gap structure. The ON/OFF current ratio increases from 6.19×10^5 for device with a-Si:H channel A (CF = 0%) to 8.30×10^5 for device with μc-Si:H channel B (CF = 28.6%), and to 7.30×10^6 for device with μc-Si:H channel C (CF = 79.3%). Here the ON/OFF current ratio is defined as the ratio of I_{ds} (ON)$|_{V_{gs}=20\,V,\ V_{ds}=1\,V}$ to I_{ds} (OFF)$|_{V_{gs}=1\,V,\ V_{ds}=1\,V}$.

Finally, the dependence of the field effect mobility (μ_{FE}) on crystalline factor (CF) of channel film is shown in Fig. 8. The H_2 gas dilution method produces high quality μc-Si:H film with less defect centers, lower optical band gap (E_{opt}) and higher crystalline factor (CF). Hence, the density of scattering center that limits the field mobility is reduced. The device performance with μc-Si:H channel film of high crystalline factor is therefore enhanced with higher field

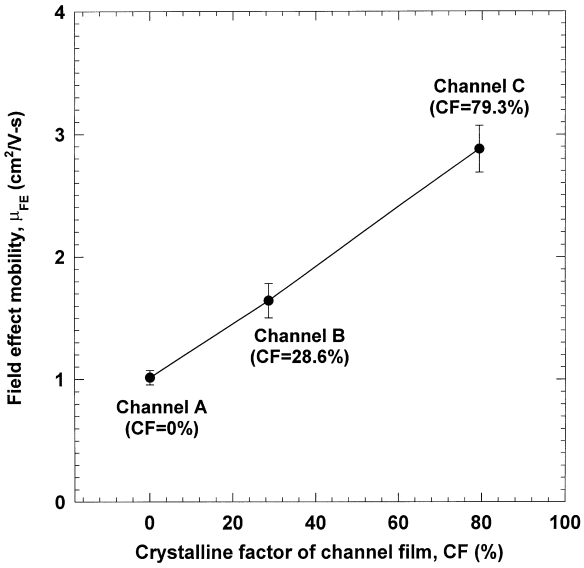

Fig. 8. Field effect mobilities for devices with channel films having various crystalline factors (CF).

effect mobility than the device with a-Si:H channel A (CF = 0%) of 1.02 cm^2/V s. Device with μc-Si:H channel C (CF = 79.3%) has a much higher field effect mobility of 2.88 cm^2/V s, while device with μc-Si:H channel B (CF = 28.6%) depicts a lower value of 1.64 cm^2/V s due to the H_2 plasma etching induced damage during the deposition. The field effect mobility was measured in the saturated region and deduced from the equation: $I_{ds} = m_{FE}$-$C_{ins}W(V_{gs} - V_{th})^2/2L$. Here μ_{FE} is the field effect mobility.

4. Conclusions

The effects of hydrogenated microcrystalline silicon film (μc-Si:H) with various crystalline factors on the performance of thin-film transistor (TFT) with low-high-low band-gap structure, which can be easily fabricated using a conventional TFT process, has been studied. A thin-film of high crystalline factor and high-band-gap is embedded vertically between the conventional a-Si:H channel and source/drain contacts in this new structure. The film of low crystalline factor and high-band-gap offset, which blocks the carrier conduction during OFF-state operation of the device, is used to prevent the band-to-band tunneling, and thus effectively reducing the large OFF-current normally observed in conventional thin-film transistors. The channel film of a high crystalline factor and low-band-gap can effectively improve the ON-state current and field-effect mobility, resulting in an overall improvement of ON/OFF current ratio.

Acknowledgements

The authors would like to express their appreciation to the staff of the Semiconductor Research Center, National Chiao Tung University for their technical support. This work was supported by the National Science Council of the Republic of China under contract No. NSC87-2215-E009-061.

References

[1] N. Ibaraki, AM-LCD'95 Dig. Japan, 1995, p. 67.
[2] Y. Kaneko, K. Tsutsui, H. Matsumaru, H. Yamamoto, T. Tsukada, IEDM Tech. Dig. (1989) 337.
[3] Y. Uchida, M. Matsumura, IEEE Trans. Electron Devices 36 (1984) 2940.
[4] Y. Uchida, Y. Nara, M. Matsumura, IEEE Electron Device Lett.5 (1984) 105.
[5] T.Y. Huang, I.W. Wu, A.G. Lewis, A. Chiang, R.H. Bruce, IEEE Electron Device Lett. 11 (1990) 244.
[6] S.S. He, G. Lucovsky, Mat. Res. Symp. Proc. 336 (1994) 25.
[7] K.C. Hsu, B.Y. Chen, H.T. Hsu, K.C. Wang, T.R. Yew, H.L. Hwang, Japan J. Appl. Phys. 33 (1994) 639.
[8] C.W. Liang, W.C. Chiang, M.S. Feng, Japan J. Appl. Phys. 34 (1995) 5943.
[9] C.C. Tsai, G.B. Anderson, R. Thompson, Mat. Res. Proc. 192 (1990) 475.
[10] C.Y. Chang, C.W. Lin, IEEE Electron Device Lett. 17 (1996) 572.
[11] C.Y. Chang, C.W. Lin, Japan J. Appl. Phys. 36 (1997) 2032.
[12] C. Y. Chang, Y. S. Lee, T. Y. Huang, P. S. Shih, C. W. Lin, Japan J. Appl. Phys., in press
[13] P.M. Garone, V. Venkataraman, J.C. Sturm, IEEE Electron Device Lett. 12 (1991) 230.